1 **Active geothermal systems with entrained seawater as analogues for low-sulphidation**

2 **epithermal mineralization**

3 Jonathan Naden,

4 British Geological Survey, Keyworth, Nottingham, NG12 5GG, UK

5 Stephanos P. Kilias

6 Department of Economic Geology and Geochemistry, University of Athens,

7 Panepistimioupolis, Zographou, 157 84, Athens, Greece

8 D.P. Fiona Darbyshire

9 NERC Isotope Geosciences Laboratory, British Geological Survey, Keyworth Nottingham,

10 NG12 5GG, UK.

11 **Abstract (207 words)**

12 The paradigm for low-sulphidation (LS) volcanic-arc associated mineralization is the active

13 geothermal systems located along the Taupo Volcanic Zone (e.g. Broadlands). However, this

14 analogue is inapt where fluid salinities are consistently in excess of 3.5 wt % NaCl.

15 LS mineralization on Milos (Aegean arc) records high paleofluid-salinities. The δD and $\delta^{18}O$

16 data do not exemplify ^{18}O-shifted meteoric waters—typical of terrestrial geothermal systems.

17 Nor is a submarine origin indicated—stable isotope data show mixing between meteoric,

18 seawater and volcanic-arc gases. Strontium isotope data are comparable to a nearby active

19 seawater-entrained geothermal system. These are features seen in hydrothermal systems

20 associated with emergent volcanoes.

21 For the Milos LS mineralization, high-salinity fluids show it cannot be explained by a

22 Broadlands-type model. The absence of saliferous sequences and significant intrusive rocks

23 preclude these as salinity sources. The similarities between paleo and active systems in terms

24 of salinity, δD–$\delta^{18}O$ and strontium isotope systematics strongly suggest that seawater is the

25 main source for Na and Cl. We suggest geothermal systems, containing seawater, associated

26 with emergent volcanoes are an alternative analogue for LS epithermal mineralization.

27 Furthermore, they bridge the gap between submarine, and large-scale terrestrial geothermal

28 systems—the modern analogues for VHMS and epithermal mineralisation in the scheme of

29 intrusion-centered hydrothermal mineralization.

30 **Keywords**

31 Epithermal processes, seawater, Milos, isotopes

Introduction

33 Geothermal systems in convergent plate margin settings are the active equivalents of high-
34 level (2–3 km) intrusion-centred hydrothermal ore-deposits (e.g. Hedenquist and Lowenstern,
35 1994). Close to magmatic activity, volcanic emanations are the surface expressions of
36 porphyry-Cu and high-sulphidation epithermal-Au mineralizing processes at depth
37 (Hedenquist et al., 1993). Located farther from the magmatic source are low-sulphidation
38 (LS) epithermal deposits, for which the Broadlands–Ohaaki geothermal system is the
39 paradigm (e.g. Simmons and Browne, 2000). Generally, in LS mineralization, fluid inclusions
40 document low-salinity fluids (< 1 wt % dissolved salts + CO_2) and these are equivalent to the
41 low-chorinity (< 1000 ppm) fluids seen in Broadlands-type geothermal systems. However,
42 they also identify saline fluids (up to 15 wt % salts) and, in this case, there are no documented
43 active analogues (Hedenquist and Lowenstern, 1994). Conversely, deep water (> 1000 m)
44 geothermal systems, such as TAG (e.g. You and Bickle, 1998) are exemplars for VHMS
45 deposits. However, where boiling submarine geothermal fluids vent into shallow water (< 200
46 m) mineralization is epithermal in style (Stoffers et al., 1999), but there are no clearly defined
47 ancient equivalents (Huston, 2000). Thus, in both the submarine and subaerial environments
48 there is a missing link between active geothermal systems and their ancient counterparts.

49 Below, we provide new strontium isotope data and summarize features of epithermal systems
50 on Milos island. By comparing these with well-characterised modern analogues we suggest
51 that active geothermal systems with entrained seawater, such as those in the Aegean arc
52 (Aegean arc-type), are an alternative to the Broadlands–Ohaaki LS paradigm in the scheme of
53 intrusion-centred hydrothermal systems.

The Aegean arc

55 The Aegean arc is a zone of Pliocene to modern volcanism related to active back-arc
56 extension caused by the subduction of the African plate beneath the Aegean micro-plate (e.g.
57 Pe-Piper and Piper, 2002). It is built on continental crust, comprises seven major volcanic
58 centres and is located 120–250 km north of the Hellenic trench (Fig. 1). The volcanic rocks
59 are calc-alkaline with localised high-K variants and range from basalt to rhyolite in
60 composition, with dominant andesites and dacites. Present day hydrothermal activity
61 comprises both low-enthalpy (Aegina, Sousaki, Methana) and high-enthalpy systems (Milos,
62 Nisyros).

63   *Milos geology and LS epithermal Au-Ag mineralization*

64   Upper Pliocene (2.66 ± 0.07 Ma; Stewart and McPhie, 2003) submarine and Late Pleistocene

65   to present (1.9–0.1 Ma) subaerial volcanic rocks overlay Mesozoic metamorphic basement

66   and Upper Miocene–Lower Pliocene marine sediments, and record a transition from a shallow

67   submarine (< 200 m) to subaerial volcanic setting (Fytikas et al., 1986; Rinaldi and Venuti,

68   2003; Stewart and McPhie, 2003). Emergence probably occurred at 1.44 ± 0.08 Ma (Stewart

69   and McPhie, 2003). Plutonic rocks are not known on Milos and have only been reported as

70   ignimbrite-hosted granitic xenoliths from the nearby islet of Kimolos (Pe-Piper and Piper,

71   2002).

72   The oldest submarine volcanic rocks occur on western Milos and host LS Au–Ag

73   mineralization (the Profitis Ilias [PI]–Chondro Vouno [CV] epithermal system), which

74   extends over a 20 km^2 area (this study; Kilias et al., 2001). Fluid inclusion data show the

75   hydrothermal fluids underwent extreme boiling and vaporisation. Importantly, final ice-

76   melting (T_{mice}) data show that 70 % of the fluid inclusions have net salinities in excess of

77   seawater (Tab. 1), showing that throughout its lifespan, fluids in the system were saline. The

78   tops of the paleosystem (now ~600 masl) show crustiform/colloform quartz–barite±alunite

79   veins and quartz-cemented breccias, with locally high gold (PI: 56 ppm; CV: 250 ppm) and

80   silver (PI: 197 ppm; CV: 90 ppm). Deeper in the system (now ~300 masl), the mineralization

81   is dominated by a base-metal-bearing stockwork. Elevated gold values at PI are concentrated

82   above the base metal zone and are spatially related to boiling (Kilias et al., 2001).

83   *Active geothermal system*

84   In the active geothermal system (Liakopoulos, 1987; Pflumio et al., 1991), data indicate a

85   two–component reservoir: (1) A high enthalpy system with deep seawater recharge located 1–

86   2 km below sea-level. Reservoir temperatures range 250–350 ºC and salinities can be

87   significantly higher than seawater (up to 9 wt % salts). This results from Rayleigh distillation

88   as seawater percolates, through progressively hotter rocks, into the reservoir. Due to its high

89   salinity, venting of the deep geothermal fluid is accompanied by boiling close to the top of the

90   reservoir and in some cases the reservoir may be two-phase. (2) A shallow reservoir (100–175

91   ºC) overlies the high-enthalpy system. It is located close to sea-level, recharged by meteoric

92   water and seawater intrusion, is commonly saline (up to 5 wt % salts) and heated by gas

93   escapes from the underlying deep reservoir. Seawater, as a major component of both the deep

94   and shallow reservoirs, is documented on the basis of $^{87}Sr/^{86}Sr$ and δD–$\delta^{18}O$–Cl systematics

95   (Pflumio et al., 1991). In the shallow (<100 m) submarine environment, venting geothermal

96   fluids contain suspended particulate matter strongly enriched in Fe, Mn, Si and Ba and locally

97   deposit APS minerals, pyrite, marcasite, barite, gypsum, and calcite (Baltatzis et al., 2001;

98   Varnavas et al., 2000). In addition, the deep reservoir is metalliferous (Pb: 180 ppb; Zn: 1458

99   ppb) (Christanis and Seymour, 1995) and has gold concentrations in the region of 0.3 ppb

100   (Liakopoulos, 1987).

101   *Strontium isotopes*

102   Sr-isotope data show that the least altered igneous rocks have low $^{87}Sr/^{86}Sr$, whereas their

103   hydrothermally altered counterparts are closer to a seawater signature (Fig. 2). The basement

104   rocks have variable strontium ratios (0.7033–0.7136)) (Fig. 2). In the modern system,

105    $^{87}Sr/^{86}Sr$ in the fluids vary from 0.7092–0.7102 (Pflumio et al., 1991). Barites from the

106   Profitis Ilias mineralization display similar $^{87}Sr/^{86}Sr$ to the modern system (Fig. 2). All values

107   for geothermal water and hydrothermal minerals are slightly more radiogenic than seawater

108   but relatively constant.

109   **Discussion**

110   *Seawater as a fluid component on Milos*

111   T_{mice} in fluid inclusions provides information on salinity. However, above −1.5 ℃, it is unable

112   to distinguish between dissolved salt (< 2.5 wt % NaCl eq.) and gas (< 4.4 wt % CO_2 eq.).

113   This permits gas-charged low-chlorinity terrestrial geothermal systems to be the paradigm for

114   LS epithermal mineralization, as excess chlorinity can be assigned to dissolved gas

115   (Hedenquist and Henley, 1985). Moreover, in Broadlands–Ohaaki-type geothermal systems

116   derivation of chlorinities in excess of 5000 ppm through fluid–rock interaction is extremely

117   difficult and where high salinities are recorded they are attributed to boiling to dryness and

118   have a localised effect (Simmons and Browne, 1997). Hence, when comparing ancient

119   systems with Broadlands–Ohaaki-type equivalents, when the apparent salinity is up to 3–4 wt

120   % NaCl eq there is an implicit requirement to assign freezing point depressions to dissolved

121   gas rather than chlorinity. However, in our case > 70 % of the fluid inclusions have net

122   salinities in excess of 3.5 wt % NaCl eq (Tab. 1). Thus, we cannot assign excess T_{mice} to

123   dissolved gas. Nonetheless, our high salinities have to be explained. There are three main

124   sodium and chlorine reservoirs available to large-scale geothermal systems: (1) evaporites and

125   evaporitic sediments (2) magmatic brines and (3) seawater. An evaporitic origin of salinity is

126   considered highly improbable, as there is no record of saliferous rocks within the Milos

127   sediments. Concerning a magmatic brine, it is estimated that during its lifetime a geothermal

128   systems turns over between $10^{6\pm1}$ km^3 of water (Barnes and Seward, 1997). If it is assumed

129   that andesitic magmas contain about 1000 ppm chlorine, then approximately $10^{7\pm1}$ km^3 of

130   magma would be required maintain salinities in the geothermal system at 9 wt % NaCl. This

131   is not impossible, but on Milos, geological and geophysical evidence is lacking (Pe-Piper and

132   Piper 2002). Thus, a magmatic origin of salinity is also considered unlikely. This leaves a

133   seawater origin for Na and Cl. We consider that the chemical similarities between the ancient

134   and modern systems on Milos (see above) support a seawater origin for the PI–CV epithermal

135   fluids.

136   Comparison of δD–$\delta^{18}O$ of inclusion fluids from the Profitis Ilias epithermal mineralization

137   and several active geothermal systems associated with emergent volcanoes reveals remarkable

138   similarities (Fig. 3). In the active systems, the geothermal fluids have a three component

139   source (sea, meteoric and magmatic) and the waters fall in a zone projecting from the

140   meteoric water line to values intermediate to seawater and volcanic-arc gases (Fig. 3). The

141   fluid inclusion data for the Profitis Ilias LS mineralization show an analogous trend and lie in

142   a similar zone; this is in sharp contrast to typical LS mineralization where stable isotope data

143   show ^{18}O-shifted fluids at constant δD (see Broadlands field in Fig. 3).

144   In terms of strontium isotope data (Fig. 2, the basement metamorphic sequence has $^{87}Sr/^{86}Sr$

145   (0.7033–0.7137) encompassing the entire range, permitting a variety of fluid–rock interaction

146   interpretations. However, we think the clustering of measured $^{87}Sr/^{86}Sr$ for the modern

147   geothermal fluids (0.7092–0.7100) and mineralization (0.7096–0.7100 [epithermal Au–Ag];

148   0.7092–0.7098 [Mn–Ba] close to the value for late-Pliocene seawater (0.7090–70906), also

149   indicates of a seawater source. In addition, as $^{87}Sr/^{86}Sr$ for the modern and ancient systems are

150   significantly different from most of the unaltered igneous rocks (0.7050–0.7080) mitigates

151   further against a magmatic fluid source. Indeed, most of the $^{87}Sr/^{86}Sr$ (0.7082–0.7098) for

152   hydrothermally altered igneous rocks cluster within or close to the range recorded by the

153   modern geothermal fluids and seawater.

154   Taken together, the above lines of evidence show that in addition to being a fundamental

155   component in the active system, seawater has played a key role in LS mineralization.

156   *Hybrid epithermal systems and modern analogues*

157   It is clear that Broadlands–Ohaaki-type meteoric geothermal systems are not a valid analogue

158   for the Milos Au–Ag mineralization and for moderately saline (> 15 000 ppm NaCl eq.) LS

159   epithermal mineralization in general. Furthermore, there is a missing link between saline

160   epithermal LS systems and their modern counterparts. We suggest that the best candidates,

161   which recognize the key parameters of consistently high fluid inclusion salinities, δD–$\delta^{18}O$

162   systematics indicating seawater and a seawater Sr isotope signature, are geothermal systems

163   with entrained seawater. Typical examples are the active systems on Milos and Nisyros (Fig.

164   3). These analogues are hybrids, containing elements of both submarine and terrestrial

165   geothermal systems. Indeed, the occurrence of fossil hybrid systems is predicted (Huston,

166   2000) though, to date, no ancient equivalents have been clearly identified. Here, in the

167   emergent environment, circulating sea and meteoric water are the main fluid components. The

168   fluids boil and result in auriferous quartz veins with epithermal textures and proximal quartz-

169   adularia, intermediate quartz–sericite–pyrite and distal propylitic/quartz–albite alteration

170   halos—features that are comparable to the Milos epithermal mineralization. Thus, we suggest

171   that epithermal mineralization where the involvement of seawater can be clearly demonstrated

172   (e.g. Milos) are good candidates for fossil hybrid epithermal systems, and active geothermal

173   systems with entrained seawater such as the Aegean-arc type, are their modern analogues.

174   Features of hybrid epithermal systems can be reconstructed by putting geothermal systems

175   associated with emergent volcanoes into a conceptual framework. Fig. 4 illustrates the

176   model—gold-bearing epithermal veins are located between a shallow low-temperature (100–

177   175 ºC) steam-heated zone recharged by meteoric water and seawater intrusion, and a deep,

178   seawater recharged, higher-temperature (250–350 ºC) base-metal bearing reservoir.

179   **Concluding remarks**

180   Broadlands-type models are not appropriate for LS epithermal systems with elevated salinities

181   that cannot be reasonably explained by dissolved gas or localised boiling to dryness.

182   Moreover, where high salinities of this nature are encountered, an explanation for them must

183   be sought. One possibility is a seawater origin for the hydrothermal fluids, though to use this

184   explanation, other parameters have to be consistent. In the case of Milos, the epithermal

185   mineralization can be explained by analogy to seawater-entrained geothermal systems

186   associated with emergent volcanoes (e.g. Nisyros, Milos) and the mineralization data

187   (geologic, isotope and fluid inclusion) are in accord with this model. We suggest that our

188   Aegean-arc model should be considered as an additional paradigm in the scheme of intrusion-

189   centred metallogenesis. Moreover, it may provide a link between submarine and terrestrial

190   mineralization processes. Appropriate indicators for its use are fluid inclusion data showing

191   consistently elevated salinities (> 3.5 wt % NaCl eq.) and mineralization hosted in submarine

192   or transitional to subaerial volcanic rocks in an island arc tectonic setting. However, it must

193   be stressed that these are not definitive and other corroborating data must be sought, in our

194   case, strontium isotope, δD and $\delta^{18}O$ analyses.

Acknowledgements

References cited

203   Baltatzis, E., Valsami-Jones, E., Magganas, A., and Kati, M., 2001, Tamarugite from Milos
204   island, Greece: Neues Jahrbuch Fur Mineralogie-Monatshefte, p. 371-377.

205   Barnes, H.L., and Seward, T.M., 1997, Geothermal systems and mercury deposits, *in* Barnes
206   Hubert, L., ed., Geochemistry of Hydrothermal Ore Deposits: New York, USA, John
207   Wiley & Sons, p. 699-736.

208   Briqueu, L., Javoy, M., Lancelot, J.R., and Tatsumoto, M., 1986, Isotope geochemistry of
209   recent magmatism in the Aegean arc: Sr, Nd, Hf, and O isotopic ratios in the lavas of
210   Milos and Santorini - geodynamic implications: Earth and Planetary Science Letters,
211   v. 80, p. 41-54.

212   Brombach, T., Caliro, S., Chiodini, G., Fiebig, J., Hunziker, J.C., and Raco, B., 2003,
213   Geochemical evidence for mixing of magmatic fluids with seawater, Nisyros
214   hydrothermal system, Greece: Bulletin of Volcanology, v. 65, p. 505-516.

215   Christanis, K., and Seymour, K.S., 1995, A study of scale deposition - an analog of
216   mesothermal to epithermal ore formation in the volcano of Milos, Aegean-arc, Greece:
217   Geothermics, v. 24, p. 541-552.

218   Farrell, J.W., Clemens, S.C., and Gromet, L.P., 1995, Improved chronostratigraphic reference
219   curve of late Neogene seawater Sr87/Sr86: Geology, v. 23, p. 403-406.

220 Field, C.W., and Fifarek, R.H., 1985, Light stable-isotope systematics in the epithermal
221 environment, *in* Berger, B.R., and Bethke, P.M., eds., Geology and Geochemistry of
222 Epithermal Systems, Volume 2: Reviews in Economic Geology, p. 99-128.

223 Fytikas, M., Innocenti, F., Kolios, N., Mannetti, P., Mazzuoli, R., Poli, G., Rita, F., and
224 Villari, L., 1986, Volcanology and petrology of volcanic products from the island of
225 Milos and neighbouring islets: Journal of Volcanology and Geothermal Research, v.
226 28, p. 297-317.

227 Giggenbach, W.F., 1992, Isotopic shifts in waters from geothermal and volcanic systems
228 along convergent plate boundaries and their origin: Earth and Planetary Science
229 Letters, v. 113, p. 495-510.

230 Hedenquist, J.W., and Henley, R.W., 1985, The importance of CO2 on freezing-point
231 measurements of fluid inclusions - evidence from active geothermal systems and
232 implications for epithermal ore deposition: Economic Geology, v. 80, p. 1379-1406.

233 Hedenquist, J.W., and Lowenstern, J.B., 1994, The role of magmas in the formation of
234 hydrothermal ore deposits: Nature, v. 370, p. 519-527.

235 Hedenquist, J.W., Simmons, S.F., Giggenbach, W.F., and Eldridge, C.S., 1993, White Island,
236 New Zealand, volcanic-hydrothermal system represents the geochemical environment
237 of high-sulfidation Cu and Au ore deposition: Geology, v. 21, p. 731-734.

238 Hein, J.R., Stamatakis, M.G., and Dowling, J.S., 2000, Trace metal-rich Quaternary
239 hydrothermal manganese oxide and barite deposit, Milos Island, Greece: Transactions
240 of the Institution of Mining and Metallurgy Section B-Applied Earth Science, v. 109,
241 p. B67-B76.

242 Huston, D.L., 2000, Gold in volcanic-hosted massive sulfide deposits; distribution, genesis,
243 and exploration, *in* S.G., H., and P.E., B., eds., Gold in 2000., Volume 13: Reviews in
244 Economic Geology, p. 401-426.

245 Kavouridis, T., Kuris, D., Leonis, C., Liberopoulou, V., Leontiadis, J., Panichi, C., La Ruffa,
246 G., and Caprai, A., 1999, Isotope and chemical studies for a geothermal assessment of
247 the island of Nisyros (Greece): Geothermics, v. 28, p. 219-239.

248 Kilias, S.P., Naden, J., Cheliotis, I., Shepherd, T.J., Constandinidou, H., Crossing, J., and
249 Simos, I., 2001, Epithermal gold mineralisation in the active Aegean Volcanic Arc:
250 the Profitis Ilias deposit, Milos Island, Greece: Mineralium Deposita, v. 36, p. 32-44.

251 Liakopoulos, A., 1987, Hydrothermalisme et Mineralisations Metalliferes de l'ile de Milos
252 (Cyclades-Grece) [PhD thesis], Paris.

253 Naden, J., Kilias, S.P., Leng, M.J., and Cheliotis, I., 2003, Do fluid inclusions preserve d18O
254 values of hydrothermal fluids in epithermal systems over geological time? Evidence
255 from paleo- and modern geothermal systems, Milos island, Aegean Sea: Chemical
256 Geology, v. 197, p. 143-159.

257 Pe-Piper, G., and Piper, D.J.W., 2002, The Igneous Rocks of Greece: Berlin, Germany,
258 Gebruder Borntraeger, 573 p.

259 Pflumio, C., Boulegue, J., Liakopoulos, A., and Briqueu, L., 1991, Oxygen, hydrogen,
260   strontium isotopes and metals in the present-day and past geothermal systems of Milos
261   Island (Aegean Arc), *in* Pagel, M., and J.L., L., eds., Source, Transport and Deposition
262   of Metals.: Rotterdam, Netherlands, A. A. Balkema, p. 107-112.

263 Rinaldi, M., and Venuti, M.C., 2003, The submarine eruption of the Bombarda volcano,
264   Milos Island, Cyclades, Greece: Bulletin of Volcanology, v. 65, p. 282-293.

265 Simmons, S.F., and Browne, P.R.L., 1997, Saline fluid inclusions in sphalerite from the
266   Broadlands- Ohaaki geothermal system: A coincidental trapping of fluids being boiled
267   toward dryness: Economic Geology, v. 92, p. 485-489.

268 —, 2000, Hydrothermal minerals and precious metals in the Broadlands-Ohaaki geothermal
269   system: Implications for understanding low-sulfidation epithermal environments:
270   Economic Geology, v. 95, p. 99-112.

271 Stewart, A.L., and McPhie, J., 2003, Facies architecture of the submarine- to subaerial
272   volcanic succession on Milos, Greece, The South Aegean Active Volcanic Arc:
273   Present Knowledge and Future Perspectives, Milos Conferences: Milos, Greece, p. 24.

274 Stoffers, P., Hannington, M., Wright, I., Herzig, P., and de Ronde, C., 1999, Elemental
275   mercury at submarine hydrothermal vents in the bay of plenty, Taupo volcanic zone,
276   New Zealand: Geology, v. 27, p. 931-934.

277 Varnavas, S.P., Panagiotaras, D., Megalovasilis, P., Dando, P., Alliani, S., and Meloni, R.,
278   2000, Compositional characterization of suspended particulate matter in Hellenic
279   Volcanic Arc Hydrothermal Centres: Physics and Chemistry of the Earth, Part B:
280   Hydrology, Oceans and Atmosphere, v. 25, p. 9-18.

281 You, C.F., and Bickle, M.J., 1998, Evolution of an active sea-floor massive sulphide deposit:
282   Nature, v. 394, p. 668-671.

283
284

284   Fig. 1. Maps showing **A)** the main geotectonic elements of the eastern Mediterranean along

285   with volcanic centres and regions of geothermal activity; **B)** the main geological features of

286   Milos island plus the location of LS epithermal mineralisation and the main surface

287   manifestations of the geothermal system (Milos map adapted from Fytikas et al., 1986; LPl:

288   Lower Pleistocene, LPo: Lower Pliocene; LMi: Lower Miocene, M: Mesozoic)

289   Fig. 2. 'S'-curve of measured strontium isotope data from mineralisation on Milos, showing

290    $^{87}Sr/^{86}Sr$ for barite, fresh and altered igneous rocks, marine platform sediments basement

291   rocks and geothermal waters (data: this study; Briqueu et al., 1986; Farrell et al., 1995; Hein

292   et al., 2000; Pflumio et al., 1991)

293   Fig. 3. Fluid-inclusion $\delta D–\delta^{18}O$ data for Profitis Ilias, comparing the epithermal

294   mineralisation with active systems on the Aegean arc with reference points for eastern

295   Mediterranean seawater (crossed squares labelled S) and estimated present day geothermal

296   liquids (filled triangles labelled M [Milos] and N [Nisyros]). (Milos epithermal mineralisation

297   data: Naden et al., 2003; geothermal data: Brombach et al., 2003; Kavouridis et al., 1999;

298   Liakopoulos, 1987; fields for volcanic arc gases and Broadlands derived from Giggenbach,

299   1992 and Field and Fifarek, 1985 respectively)

300   Fig. 4. Conceptual model of hybrid Aegean-arc-type epithermal systems (adapted from

301   Kavouridis et al., 1999; Liakopoulos, 1987)

302

302

303

304

305

306

307

308

309

310
311
312

TABLE 1. SUMMARY SALINITY DATA FOR PI–CV
EPITHERMAL AU–AG MINERALISATION

Deposit	Salinity (wt % NaCl eq.)				% FI with Tmice
	n	Min.	Max.	Mean	σ	< -2.5 ºC
*CV	132	0.5	14.7	6.1	3.0	86%
†PI	139	0.0	11.3	5.2	2.1	71%

*this study
†Kilias et al., 2001

313
314
315

316

317
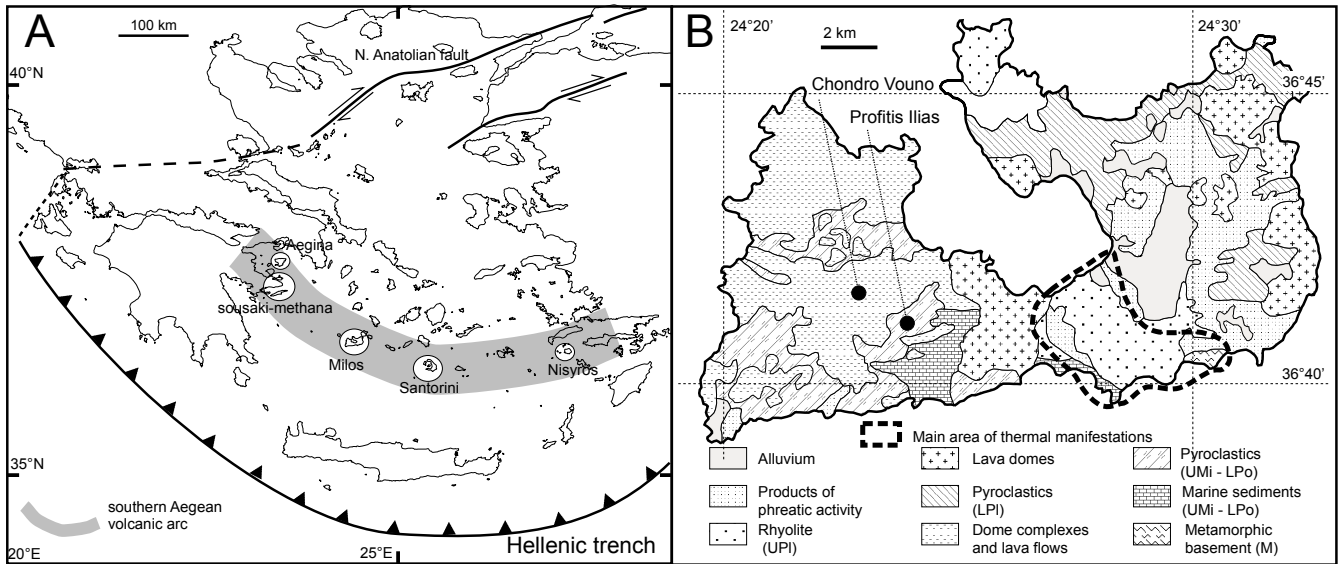
Naden et al: Geology, Fig. 1, actual size
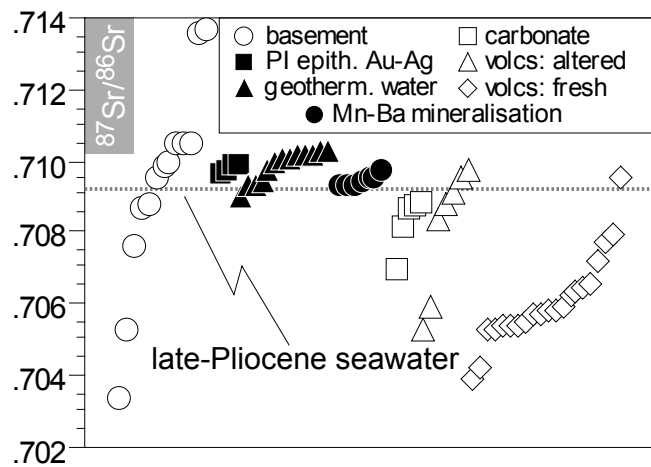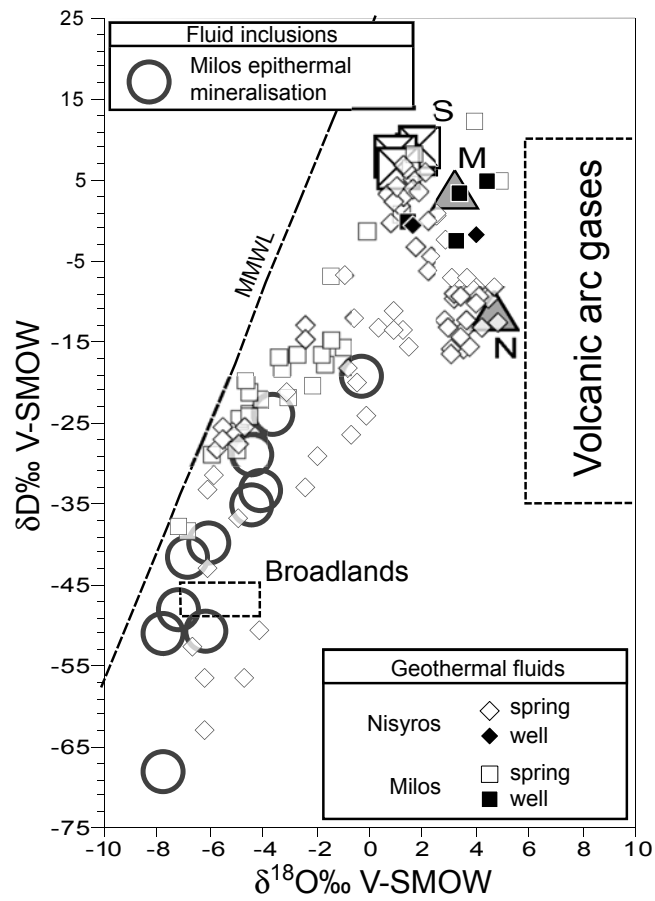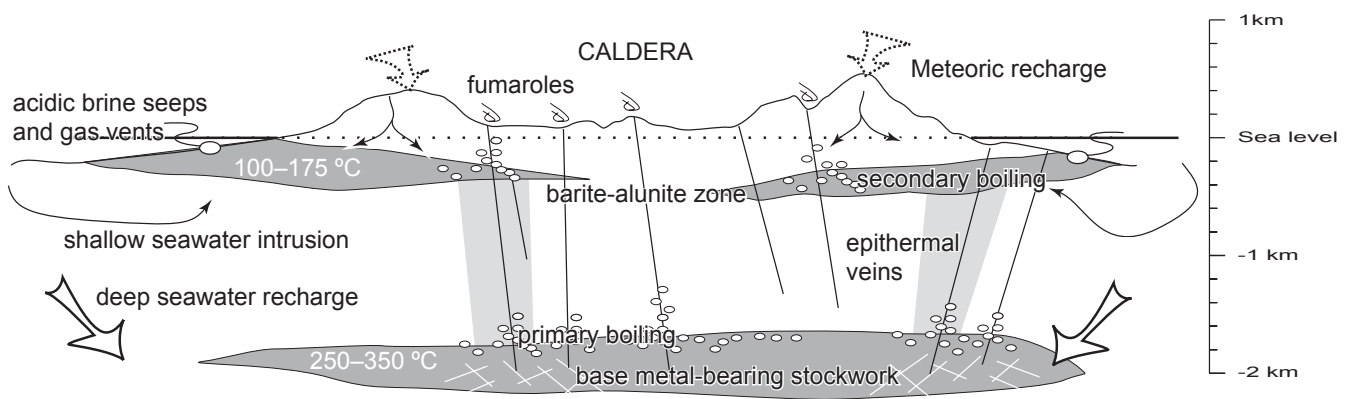
Naden et al: Geology, Fig. 2, actual size

Naden et al: Geology, Fig. 3, Actual size

Naden et al: Geology, Fig. 4, actual size